Available online at www.sciencedirect.com

ScienceDirect

Journal of Nutritional Biochemistry 26 (2015) 1174–1182

Journal of Nutritional Biochemistry

Effects of dietary resveratrol on excess-iron-induced bone loss via antioxidative character

Lu Zhao[a,1], Yin Wang[b,1], Zejian Wang[a], Zheng Xu[c], Qiaoyan Zhang[d,*], Ming Yin[a,*]

[a]School of Pharmacy, Shanghai Jiaotong University, Shanghai 200240, China
[b]People's Liberation Army 455 Hospital, Shanghai 200050, China
[c]Changzheng Hospital, Shanghai 200003, China
[d]School of Pharmacy, Second Military Medical University, Shanghai 200433, China

Received 3 September 2014; received in revised form 29 April 2015; accepted 12 May 2015

Abstract

Estrogen deficiency has been considered to be a major cause of osteoporosis, but recent epidemiological evidence and mechanistic studies have indicated that aging and the associated increase in reactive oxygen species (ROS) are the proximal pathogenic factors. Through ROS-mediated reactions, iron can induce disequilibrium of oxidation and antioxidation and can cause bone loss in mice. Therefore, we investigated the effects of resveratrol (RES) on bone mineral density, bone microstructure and the osteoblast functions under iron-overload conditions. Excess iron disrupted the antioxidant/prooxidant equilibrium of the mice and induced the defect and the lesion of the bone trabecula as well as disequilibrium between bone formation and bone resorption in iron-overload mice. Oral administration of RES significantly prevented bone loss in the osteoporotic mice. RES reversed the reduction of Runx2, OCN and type I collagen from excess iron; up-regulated the level of FOXO1; and maintained the antioxidant/prooxidant equilibrium in the mice. RES also reduced the ratio of OPG/RANKL in MC3T3-E1 cells and in mice and significantly inhibited subsequent osteoclastogenesis. These results provide new insights into the antiosteoporosis mechanisms of RES through antioxidative effects, suggesting that RES can be considered a potential natural resource for developing medicines or dietary supplements to prevent and treat osteoporosis.

Keywords: Osteoporosis; Iron overload; Resveratrol; Antioxidant effect; Sirt 1

1. Introduction

Osteoporosis is a progressive bone disease caused by aging, estrogen deficiency and genetic factors and is characterized by bone mass decline and trabecular architecture deterioration that results in fragility fractures [1]. Estrogen deficiency has been considered to be a major cause of osteoporosis in both women and men. Even though hormone replacement therapy is partially effective at slowing bone loss in postmenopausal women, a substantial number of women have discontinued its use because of the concerns about the potential risks (especially breast cancer) [2,3].

From the view of osteoporosis pathogenesis, women experience not only estrogen deficiency but also iron accumulation as a result of ceasing menstruation [4]. Men older than 40 years are at high risk for iron loading [5]. Osteoporosis and fractures occur frequently in disorders associated with iron overload, such as thalassemias and hereditary hemochromatosis [6].

Previous studies have suggested that increased oxidative levels are associated with aging in both elderly people and OVX rats and that increased iron plays a causal role in osteopenic development [7]. Iron is critical for cell growth, oxygen utilization, various enzymatic activities and responses of immune systems, but abnormal iron uptake causes widespread organ damage including liver, adrenal glands, heart, pancreas and bone [8,9]. Iron occurs in the +II and +III oxidative states, and the ferrous ions are unstable in aqueous media and tend to catalyze the generation of damaging reactive free radicals via Fenton reaction [8]. Through reactive oxygen species (ROS)-mediated reactions, iron can disrupt the antioxidant/prooxidant equilibrium of cells and can cause indirect DNA damage, lipid peroxidation and protein modification. Therefore, oxidative damage and the dysfunction of antioxidant system are the proximal pathogenesis of male and female osteoporosis. In an iron-overload male mice model, administration of iron dextran increased the level of ROS and the phosphorylation of $p66^{shc}$ (an amplifier of H_2O_2 generation in mitochondria) in bone and caused trabecular and cortical thinning, while the bone loss was largely prevented by treatment with the antioxidant *N*-acetyl-L-cysteine (NAC) [6]. $p66^{shc}$ is a crucial mediator of the effects of oxidative stress on osteoblast apoptosis, NF-κB activation and production of cytokines, such as TNF-α and IL-6 [10]. Upon oxidative stress, $p66^{shc}$ is phosphorylated at Ser36, contributing

* Corresponding authors.
E-mail addresses: zqy1965@163.com (Q. Zhang), myin@sjtu.edu.cn (M. Yin).
[1] These authors contributed equally.

http://dx.doi.org/10.1016/j.jnutbio.2015.05.009
0955-2863/

to inactivation of the winged forkhead transcription factors FOXO1, FOXO3, FOXO4 and FOXO6, which maintain skeleton genesis. Extensive research has shown that FOXOs control the regulation of many genes involved in the cell cycle, stress response, cell death, modulation of inflammation, metabolism, protection from oxidative stress and cell survival, and FOXO1 has been demonstrated to be a major regulator of osteoblast function [11].

Resveratrol (RES) is a member of the stilbene family of phenolic compounds. The major dietary sources of RES include peanuts, pistachios, berries, dark chocolate and grapes as well as their derivatives. Grapes have the highest content, while red wine is the most notable dietary source [12]. Many reports have shown that RES can prevent or slow the progression of a wide variety of illnesses, including skeletal diseases, cancer, cardiovascular disease and ischemic injuries, as well as can enhance the resistance to stress and extend the lifespan of various organisms. The major impacts are antioxidative, antiinflammatory, cardioprotective, antiaging as well as anticancer and chemopreventive [13]. Sirtuin1 (Sirt1), an NAD^+-dependent deacetylase and a key player in aging and metabolism, has been shown to regulate bone mass [14]. As a natural Sirt1 agonist, RES can up-regulate the level of FOXOs and increase the activities of antioxidant enzymes in C2C12 mouse myoblasts cells and human monocytic THP-1 cells under oxidative stress conditions [15,16]. Researchers have demonstrated that RES supplementation can promote osteogenic differentiation of modulation of Sirt1/Runx2 mediated by mesenchymal stem cell, increase the levels of osteocalcin and alkaline phosphatase (ALP) in plasma and ameliorate the loss of femur strength in hindlimb-suspended old male rats [17,18]. However, the relevant molecular mechanisms of RES and the regulation of FOXOs on bone and osteoblasts damage induced by iron overload remain unclear. In this study, we investigated the effect of dietary RES on excess-iron-induced bone loss and the potential proximate mechanisms.

2. Materials and methods

2.1. Chemicals

The mouse antiosteocalcin (OCN) antibody was purchased from Millipore (Bedford, MA). The mouse anti-FOXO1 antibody was purchased from Cell Signaling Technology (Beverly, MA), and other antibodies were purchased from Abcam (Cambridge, MA). RES, NAC, ferric ammonium citrate (FAC) and all other chemicals were purchased from Sigma.

2.2. Animals

2.2.1. Ethics

All of the experimental procedures in this study were approved by the Animal Ethics Committee of the Shanghai Jiao Tong University. The care and use of animals were conducted under the Guidelines for Animal Experiment of the Shanghai Jiao Tong University (Approval No. SYXK 2012-0017, Shanghai, China), and all efforts were made to minimize suffering.

2.3. In vivo study design

Sixty 2-month-old C57/BL6 male mice were randomly divided into six groups with ten mice each group: control group; model group; positive drug (NAC, 100 mg/kg, ig per day) group; low-dose RES group (30 mg/kg, ig per day); middle-dose RES group (60 mg/kg, ig per day); high-dose RES group (90 mg/kg, ig per day). The experimental animals were housed in hygienic plastic cages in a clean well-ventilated room and were given free access to food and water with normal light and dark cycles. The mice in the model group and the groups administered RES were treated once a week for 3 months with intraperitoneal iron dextran (100 mg/kg) or placebo (in the normal group). Three months later, the mice were killed. An hour after the last RES or placebo treatment, blood was collected to measure the cytokines and the plasma levels of RES. The femurs and livers were collected for micro-computed tomography (micro-CT) scanning, mechanical testing or an antioxidant enzyme assay.

2.3.1. Micro-CT

After removing the soft tissues, the left femurs of the mice were placed in a phosphate-buffered saline (PBS) buffer with 10% formaldehyde. The femurs were placed with gauze in the sample holder and were scanned using the GE Healthcare Locus SP micro-CT (GE Healthcare, USA) using a resolution of 6 μm, 80 kV, 80 μA, 400 number of views and exposure of 5 h [19]. The explore reconstruction utility software (GE Healthcare, USA) was used for three-dimensional reconstruction and data processing. A global threshold was defined as the lowest mineral density. Calculation methods of bone parameters have been previously described [20]. The volumetric parameters of bone volume fraction (BVF), trabecular thickness (μm), trabecular number (no./mm), trabecular spacing (μm) and the thickness and area of cortices were assessed to investigate the effect of NAC and RES on the microarchitecture of the cortical bone at mid-diaphysis femur and trabecular bone from distal femur.

2.3.2. Mechanical testing

Three-point bending testing was performed using a Dynamic Mechanical Analyzer (Shimadzu, Japan) to determine the material properties (elastic load, maximum load, elastic stress, maximum stress and modulus of elasticity) of the bones. The right femurs of the mice were thawed to room temperature and kept moist in PBS. The right femurs were loaded to failure in three-point bending with a span length of 6 mm at a rate of 0.1 mm/s until the moment of fracture [21]. The obtained load–time curve was converted into a load displacement curve, and elastic load, maximum load, elastic stress, maximum stress and elastic modulus were calculated according to formulas [22].

2.3.3. Antioxidant enzyme assay

Oxidative stress was defined as an imbalance between antioxidant systems in the body and free radical production caused the lipid peroxidation in lipid bilayers of cells. Recent clinical, epidemiological and mechanistic evidence has indicated that aging and the associated increase in ROS are the proximal culprits of osteoporosis [23]. The activities of antioxidant enzymes such as catalase (CAT), superoxide dismutase (SOD) and glutathione peroxidase (GPx) and the concentration of malondialdehyde (MDA) in liver reflect the conditions of oxidative stress and oxidative damage caused by iron overload. Liver samples were quickly excised and washed in ice-cold PBS, dried using filter paper and weighed. They were then homogenized in 4 volumes of Tris–HCl buffer and then centrifuged at 5000g for 15 min. The supernatant was collected and determined within 2 h. SOD activity was determined by inhibiting autocatalytic adrenochrome formation at 480 nm. CAT activity was determined by the changes in absorbance that were recorded at 240 nm, calculated in terms of micromoles of H_2O_2 consumed per minute per milligram of protein. GPx activity was assayed by measuring the glutathione disulfide reduction (per minute per milligram of protein) mediated by NADPH oxidation at 340 nm. Lipid peroxidation was assayed by measuring the level of MDA using the method of Ruiz-Larrea *et al.* [24].

2.4. Cell experiments

2.4.1. Cell lines and culture conditions

MC3T3-E1 cells derived from newborn mouse calvaria were purchased from the typical Culture Collections Committee cell library of the Chinese Academy of Sciences (Shanghai, China). MC3T3-E1 cells were maintained in dishes (55 cm^2) in α-MEM containing 10% fetal bovine serum (FBS) in a humidified atmosphere of 5% CO_2 in air at 37°C.

2.4.2. Cell treatment

Cells were harvested when they reached approximately 80% confluence and were randomly divided into the following six groups: a normal control group, a FAC group, three RES groups (2, 10 and 50 μM) and NAC (1 mM) group. To prove the relationship between activation of Sirt1 and promotion of RES on bone formation, MC3T3-E1 cells were treated with 50 μM RES and 5 μM EX-527 (a Sirt1 inhibitor, IC_{50} of 38 nM) [25].

2.4.3. Cell proliferation

To evaluate the effect of iron overload on osteoblast proliferation, the MC3T3-E1 cells were suspended in complete medium and plated in 96-well culture plates (Nunc, Denmark) at a density of 10^4 cells per well and incubated overnight in 10% FBS medium. Then, the cells were subjected to FAC, and cell proliferation was measured using an MTT assay after incubation for 24, 48 and 96 h at 37°C [26]. The toxicity of RES (2–1000 μM, for 48 or 72 h) was determined by MTT assay. After each cell group establishment, 20 μl MTT solution (5 mg/ml) diluted in PBS was added to each well of culture plates, and the cultures were immediately incubated for 4 h at 37°C. The medium was then removed, and 200 μl of DMSO was added to each well. Later, the plates were shaken for 10 min at room temperature and read on a microplate reader at a wavelength of 570 nm.

2.4.4. ALP assay

ALP activity was determined according to a method reported previously. MC3T3-E1 cells were suspended in complete medium and plated in 24-well culture plates at a density at a density of 5×10^4 cells per well and incubated overnight. The cells were cultured with NAC (1 mM) and RES (2, 10 and 50 μM). After 2 h, the cells were subjected to FAC (500 μM) for 3 days. After incubation, the medium was removed, and the cells were gently washed twice with PBS, scraped into 0.2% Triton X-100 and incubated at 37°C for 30 min. The lysed cells were centrifuged at 12,000 rpm for 5 min at 4°C. The supernatant was used to measure intracellular ALP activity and total protein content according to a method reported previously [27]. ALP activity was measured using an ALP activity assay kit (Jiancheng, Nanjing, China).

2.5. Western blotting and ELISA analysis

Bone extracts were prepared by extracting frozen pulverized bone tissue and suspending in RIPA buffer with a mixture of protease inhibitor cocktail and phosphatase inhibitor cocktail (Roche Diagnostics) [28]. MC3T3-E1 cells were plated in 6-well plates after overnight incubation at 37°C at a density of 1×105 cells per well. The cells were cultured with NAC (1 mM) and RES (2, 10 and 50 μM). After 2 h, the cells were subjected to FAC (500 μM) for 48 h. The cells were collected using a rubber scraper, and proteins were extracted with RIPA buffer. The proteins from the vertebrae of mice or MC3T3-E1 cell concentration were determined by a BCA protein assay kit (Jiancheng, Nanjing, China). Protein (20–30 μg) was loaded onto a 12% gel using 25 μg of protein per lane and transferred to PVDF membranes. After blocking, the membranes were incubated with primary antibodies overnight at 4°C, washed with PBST (0.1% Tween-20) and incubated for 1 h with the corresponding secondary antibody conjugated with horseradish peroxidase. The membranes were washed three times with PBST and visualized using an enhanced ECL chemiluminescent western blotting detection system (Millipore, USA). The band density was quantified using Image J soft (LI-COR Biosciences). The level of OCN in MC3T3-E1 cells and the serum concentrations of bone resorption markers including TRACP-5b, IL-6 and TNF-α were assayed using an ELISA kit (Jiancheng, Nanjing, China). Assays were performed according to the manufacturer's recommendations.

2.6. Blood RES concentrations detected by UPLC/MS/MS

Before analysis, the plasma samples were thawed to room temperature. Plasma (100 μl) was added by 400 μl acetonitrile (4:1, v/v), and vortex was mixed for 1 min. After centrifugation at 14,000 rpm for 10 min, an aliquot of 2 μl supernatant was injected into the UPLC/MS/MS system. The UPLC/MS/MS system is consisted of a Waters UPLC system with an API5500 triple-quadrupole mass spectrometer (Applied Biosystems/SCIEX, Concord, Canada) and equipped with a turbo ion spray source. Chromatographic separation was achieved with an Agilent C18 column (50 mm×2.1 mm ID, 5 μm; USA) and the oven temperature was maintained at 45°C. Electrospray ionization (ESI) was performed in negative mode with nitrogen as the nebulizing turbo spray. The nebulizer temperature was set at 600°C and the ESI needle voltage was adjusted to −5000 V. Multiple reaction monitoring detection was employed using nitrogen as the collision gas (5 arbitrary units); the precursor/product ion pairs monitored were 227.1→143.0 for RES.

2.7. Statistical analysis

Data are expressed as the mean±S.D. of at least three independent experiments. One-way analysis of variance followed by Dunnett's *t* test was used for the statistical analysis (SPSS 13.0 software; SPSS, Chicago, USA). A *P* value of <.05 was conventionally considered to be statistically significant. Graphs were drawn using GraphPad Prism (version 6.0 for Windows).

3. Results

3.1. The effect of RES on bone mineral density (BMD) and bone structural properties of the femurs

The micro-CT images of distal femoral diaphysis clearly showed the morphology of trabecular bone in the femur of the mice (Fig. 1). Following iron dextran administration over a period of 90 days, the mice injected with iron dextran in model group had a noticeable decrease in BMD at the femoral neck compared with the mice in control group (Fig. 1B and Table 1). As a positive control, NAC (Fig. 1C and Table 1) led to an obvious increase in trabecular bone density. All of the mice administered various amounts of RES demonstrated a higher density in cancellous bone tissues compared with the iron-overload mice (Fig. 1D–F and Table 1). However, the assay revealed that excess iron significantly decreased bone parameters, including BV/TV and trabecular number, with a concomitant increase in trabecular spacing. RES treatment (especially in the high-dose group) improved bone density and decelerated the degeneration of trabecular bone; significantly increased BVF, trabecular thickness and trabecular number; and decreased trabecular separation compared with model controls (Table 1). Based on an analysis of cortical bones at the mid-diaphysis femur, the mice in the model group showed thinner cortices and decreased cortical areas compared with normal controls. Micro-CT examination of cortical bone revealed a remarkable effect of RES on the femur of iron-overload mice. Out of all the oral administration results, 90 mg/kg RES per day led to the best effect, which was also better than the positive control group administered NAC.

3.2. The effect of RES on mechanical properties of the femurs

The results obtained from the three-point bending test showed that the mice from the model group had significantly reduced elastic load, maximum load, elastic stress, maximum stress and elastic modulus of the femurs. When administered 90 mg/kg RES per day, the mice showed significant ($P<.05$) improvements in all parameters related to bone strength compared with the model controls. In addition, RES protected against the destructive effects of iron overload on mechanical properties of the femurs in a dose-dependent manner (Fig. 2). Obviously, administration of RES significantly improved the bone mechanical strength and led to a lower risk of fracture in an iron-overload osteoporosis model.

3.3. The effect of RES on the serum levels of TRACP-5b, IL-6 and TNF-α

As shown in Fig. 3, the serum levels of the osteoclast activity markers (TRACP-5b, IL-6 and TNF-α) were significantly higher in the model group than in the normal group. Our data showed that RES treatment reduced the levels of osteoclast activity markers such as IL-6, TNF-α and TRACP-5b and maintained normal osteoblast activity levels. These findings suggest that RES significantly inhibits osteoclastogenesis and protects against osteogenesis in the osteoporotic mice induced by iron overload.

3.4. The effect of RES on protein expression in MC3T3-E1 cells and the mouse femur

In animal experiments, western blot analysis (Fig. 4A) showed that Runx2, osteocalcin (OCN) and type I collagen (Col I) protein expression levels in the model group were significantly lower compared with the normal group. Mean data and a representative gel showed that RES and NAC reversed the iron-overload-induced, down-regulated expression of OCN and Col I. *In vitro* treatment with FAC for 48–96 h led to no significant difference in cell viability between the iron-overload group and normal group (Fig. 4B). However, the ALP activity and the levels of OCN were significantly reduced by excess iron treatment. Interestingly, pretreatment with RES (2–50 μM) for 2 h significantly protected osteoblasts against a dose-dependent reduction in ALP and OCN induced by excess iron (500 μM). EX-527, a Sirt1 inhibitor used in many physiological studies at 5 μM, reversed the effect of RES on osteogenesis in MC3T3-E1 cells, indicating the effects of RES on osteogenesis mediated, at least in part, by activation of Sirt1 (Fig. 4C and D) [29].

We examined the effects of RES on the expression of RANKL (receptor activator of nuclear factor κ B ligand) and OPG (osteoprotegerin) in mice and MC3T3-E1 cells under iron-overload conditions. As shown in Fig. 5A and B, treatment with excess iron dramatically increased the ratio of RANKL/OPG in iron-overload mice and MC3T3-E1 cells. RES was also shown to maintain a normal RANKL/OPG balance, avoiding excessive activation of osteoclasts induced by excess iron. These data were consistent with the results for serum levels of TRACP-5b, IL-6 and TNF-α. Together, these findings in mice and osteoblasts suggest that RES inhibited osteoclastogenesis via a RANKL/OPG signaling pathway.

3.5. The antioxidant effect of RES in iron-overload MC3T3-E1 cells and mice

As iron is mainly cleared by liver macrophages, the liver is the most important organ to store excess iron, and the subsequent accumulation of iron in the liver leads to oxidative stress in iron-overload conditions [30]. The activities of antioxidative enzymes in livers are

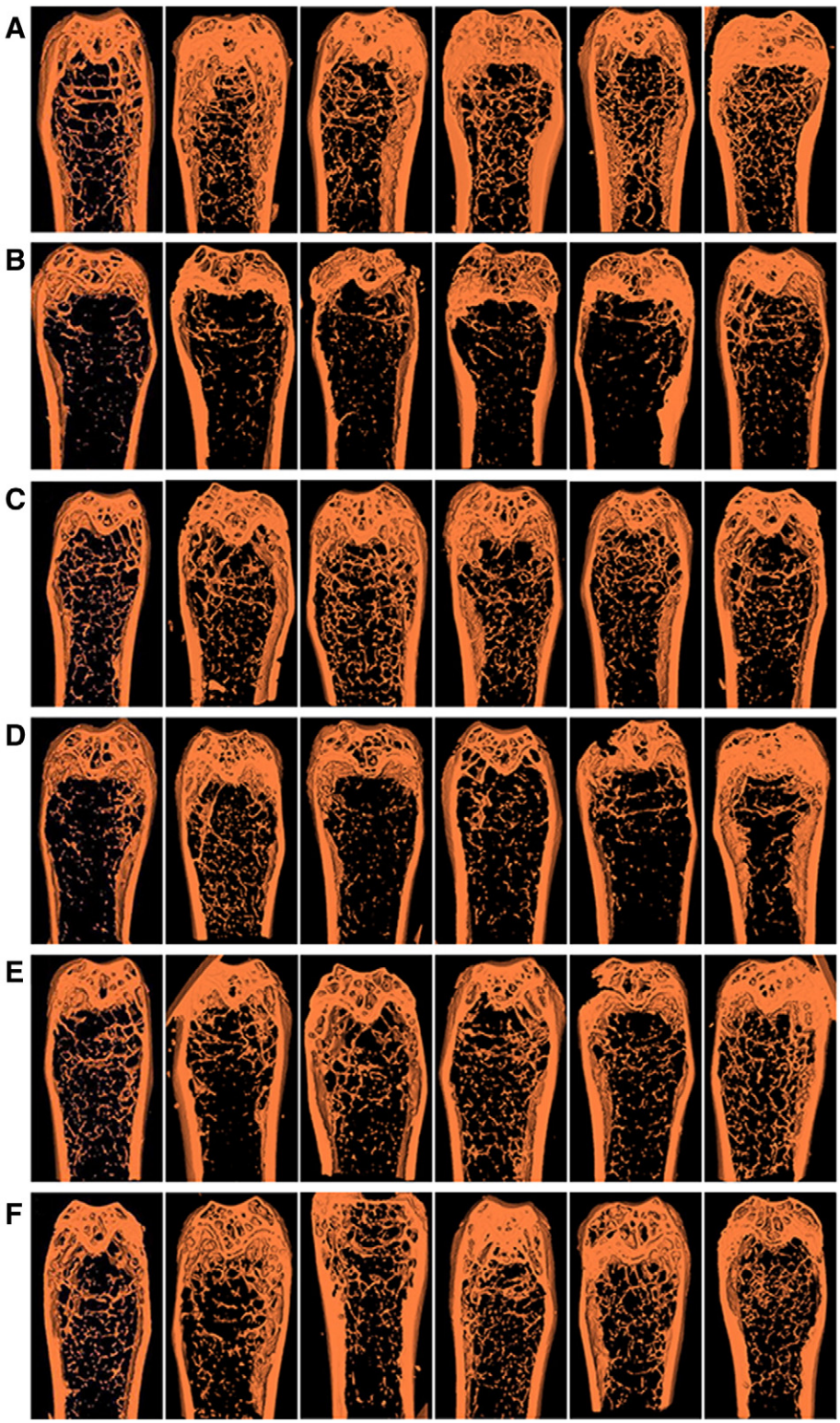

Fig. 1. The effect of RES on BMD and bone structural properties of the femurs. Representative three-dimensional reconstructed images derived by micro-CT in the control group (A), iron-treated group (B), NAC+iron-treated group (C), 10 mg/kg RES+iron-treated group (D), 30 mg/kg RES+iron-treated group (E) and 90 mg/kg RES+iron-treated group (E).

sensitive indicator of oxidative stress induced by iron overload. As showed in Fig. 6A, the activities of the antioxidative enzymes CAT, SOD and GPx in liver were significantly decreased, and the level of MDA was significantly elevated in mice from the model group. NAC supplementation preserved the antioxidant activities and decreased MDA content. Administration of RES significantly restored hepatic CAT, SOD and GPx and decreased the level of MDA. FOXO1 transcriptional factors are critical regulators in response to oxidative stress in osteoblasts and an animal model of osteoporosis [31]. As shown in Fig. 6B and C, treatment with iron dextran significantly

Table 1
Micro-CT analysis of mice treated with placebo, iron dextran and iron dextran+RES

	Placebo	Iron	Iron+NAC	Iron+RES10	Iron+RES30	Iron+RES90
Trabecular bone						
BMD, mg/mm^3	304.74±46.98	179.62±23.72[a]	257.40±29.43[b]	198.03±11.22	216.33±14.93	270.73±31.27[c]
BVF, percentage	24.9±7.4	11.5±2.0[a]	21.0±3.3[b]	11.8±2.5	13.0±1.9	24.1±4.4[c]
Trabecular number, N/mm	5.58±1.26	3.54±0.34[a]	4.83±0.77[b]	3.71±0.55	3.83±0.42	5.59±0.67[c]
Trabecular thickness	44.41±7.59	32.23±2.94[a]	43.33±2.21[c]	31.54±2.36	33.66±1.73	43.34±8.89[b]
Trabecular spacing	142.20±43.73	252.43±31.56[a]	167.75±34.81[c]	242.62±46.26	229.71±32.34	131.20±18.65[c]
Cortical bone						
Cortical thickness, mm	0.134±0.006	0.118±0.005[a]	0.133±0.004[c]	0.122±0.014	0.122±0.005	0.123±0.006[b]
Cortical area, mm^2	0.801±0.034	0.609±0.023[a]	0.733±0.021[c]	0.672±0.152	0.737±0.031	0.816±0.089[c]
Marrow area, mm^2	1.208±0.011	1.342±0.056[a]	1.257±0.033[b]	1.303±0.137	1.264±0.134	1.183±0.009[c]

Results are represented as the mean±S.D. (n=6).
[a] P<.05 compared to the control group.
[b] P<.05 compared to the iron-treated group.
[c] P<.01 compared to the iron-treated group.

increased the phosphorylation of p66^{shc} and inhibited the expression of FOXO1 in the femur and MC3T3-E1 cells, whereas administration of RES reversed excess-iron-induced inhibition of FOXO1 and inhibited the phosphorylation of p66^{shc} to reduce the oxidative damage.

3.6. The vitro cytotoxicity and plasma levels of RES

As shown in the Fig. 7A, RES (1000 μM) significantly caused MC3T3-E1 cell death (P<.05). There were no statistically significant differences in cell viability between treatment with RES groups (2–500 μM, for 48 or 72 h) and control group. As shown in the Fig. 7B, the plasma levels of RES of three different dose groups varied considerably. The differences in plasma levels of RES among groups treated with 90, 30 or 10 mg/kg RES resulted in varying efficacy to bone loss induced by excess iron.

4. Discussion

Estrogen deficiency has been considered to be a major mechanism of osteoporosis in both women and men, but epidemiological evidence and recent mechanistic studies have indicated that aging and the associated increase in ROS are the proximal pathogenesis. Loss of estrogen or androgen decreases the defense against oxidative stress in bone, and this loss accounts for increased bone resorption associated with the acute loss of these hormones. In addition to estrogen deficiency, women during menopause experience a 2- to 3-fold iron

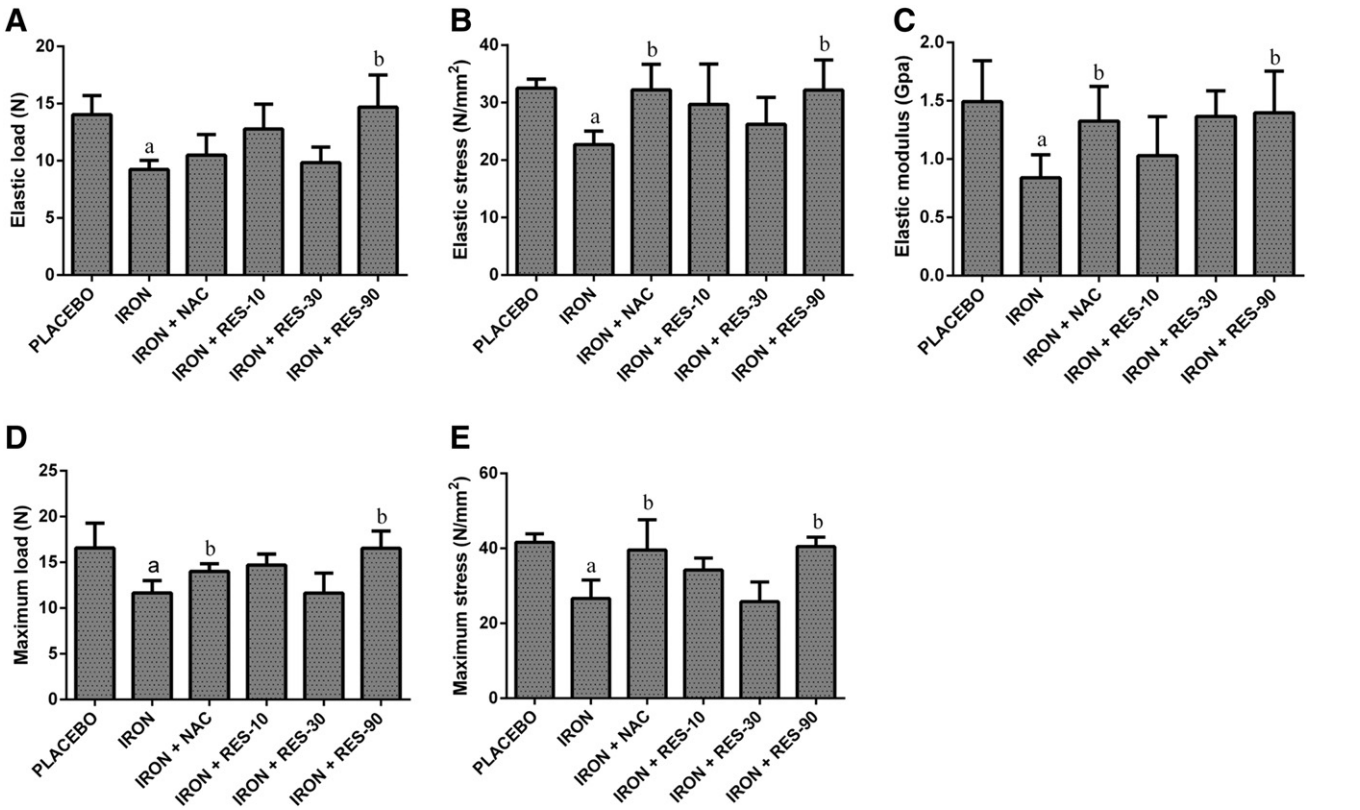

Fig. 2. The effect of RES on mechanical properties of the femurs. Elastic load (A), elastic stress (B), elastic modulus (C), maximum load (D) and maximum stress (E) of the femurs were derived from the three-point bending test. Results are represented as the mean±S.D. (n=6) a: P<.05 compared to the control group; b: P<.05 compared to the iron-treated group; c: P<.01 compared to the iron-treated group.

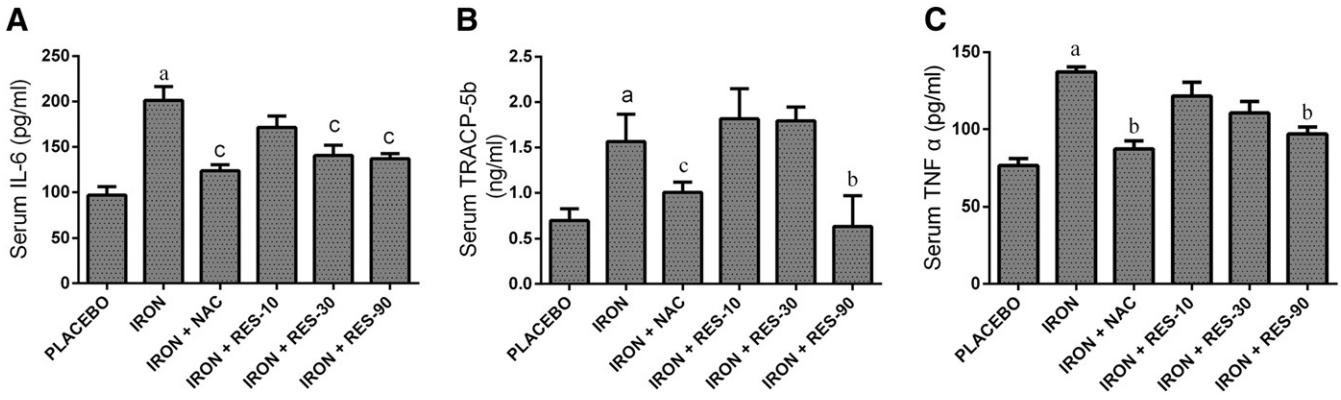

Fig. 3. The effect of RES on the serum levels of TRACP-5b, IL-6 and TNF-α. The serum concentrations of bone resorption markers including IL-6 (A), TRACP-5b (B) and TNF-α (C) were assayed using an ELISA kit. Results are represented as the mean±S.D. (n=8) a: P<.05 compared to the control group; b: P<.05 compared to the iron-treated group; c: P<.01 compared to the iron-treated group.

increase as a result of cessation of menstruation [4]. Men older than 40 years are also at high risk for iron loading [5]. In male mice model, excess iron increased bone resorption and oxidative stress, leading to changes in bone microarchitecture [6]. Iron chelation with desferrioxamine inhibited osteoclastogenesis and the acceleration of bone resorption and significantly improved pathological changes in microstructure of bone [32]. Treatment with FAC (500 or 1000 μM) for 48–96 h had no significant difference of cell viability but inhibited the progress of bone formation by reducing Runx2, OCN and Col I protein expression levels between iron-overload group and normal group in MC3T3-E1 cells. It was different from other oxidative stress damage cell model in rat calvarial osteoblast or MC3T3-E1 (unpublished data) induced by H_2O_2 in our other studies.

Iron can induce up-regulation of ferritin, and the inhibition of osteoblast activity, mineralization and specific gene expression is attributed to the ferroxidase activity of ferritin [33]. In our study, the mice administered RES demonstrated a higher density in cancellous bone tissues compared with the iron-overload mice. The micro-CT images of distal femoral diaphysis showed that only the higher dose appears significantly beneficial on BMD and bone structural properties. However, RES significantly reversed iron-overload-induced, down-regulated expression of OCN and Col I in dose-dependent manners. The prolonged time of administration of middle and low dosage may appear beneficial on enhancement of bone mass and improvement of bone quality. Runx2 directs preosteoblast cells into immature osteoblasts, which then leads to promoter activation and

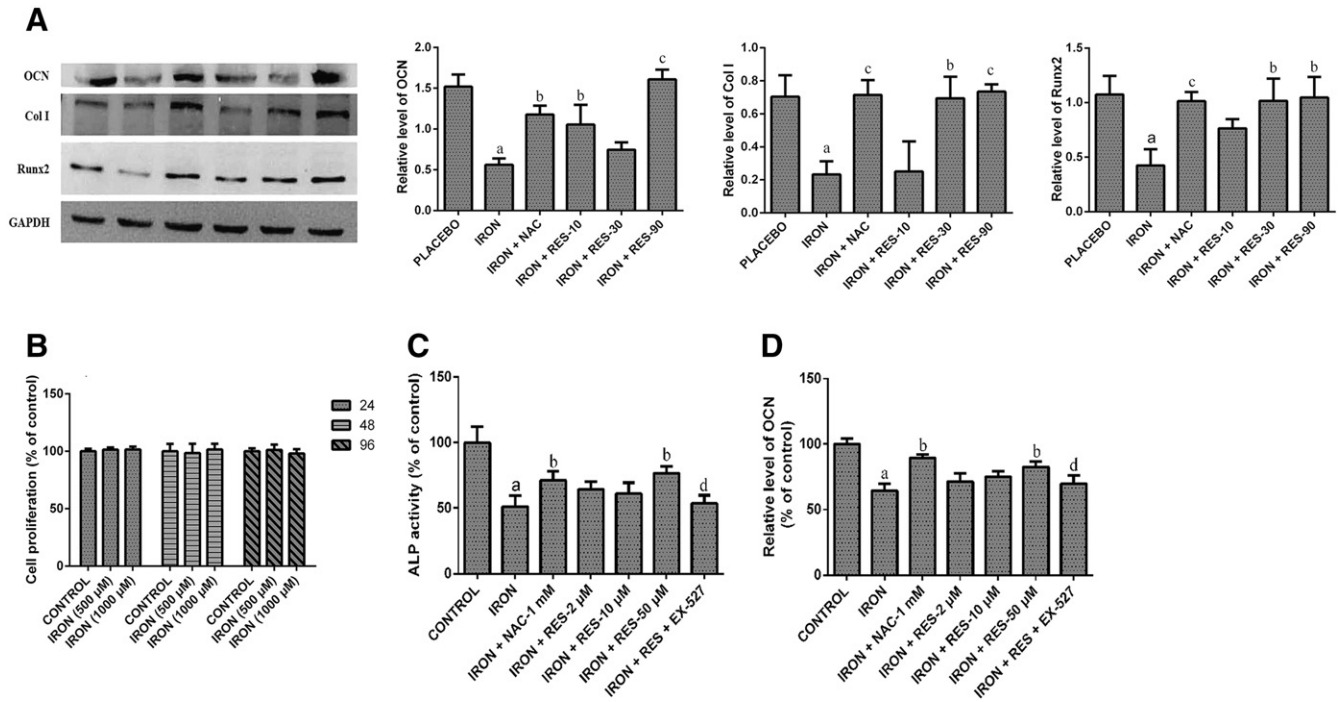

Fig. 4. The effect of RES on osteogenesis of iron-overload mice and MC3T3-E1 cells. Bone extracts were prepared by extraction of frozen pulverized bone tissue and suspended in RIPA buffer. Proteins were subjected to western blotting assay for the expressions of OCN, Col I and Runx2 (A). MC3T3-E1 cells were treated with iron (500 or 1000 μM), and the cell proliferation was measured by MTT assay after incubation for 24, 48 and 96 h (B). (n=10). MC3T3-E1 cells were cultured with NAC (1 mM) and RES (2, 10 and 50 μM). After 2 h, the cells were subjected to FAC for 48 h. ALP activity (C) was measured using an ALP activity assay kit. The level of OCN (D) was assayed using an ELISA kit. Results are represented as the mean± S.D. (n=5) a: P<.05 compared to the control group; b: P<.05 compared to the iron-treated group; c: P<.01 compared to the iron-treated group; d: P<.05 compared to 50 μm RES+iron-treated group.

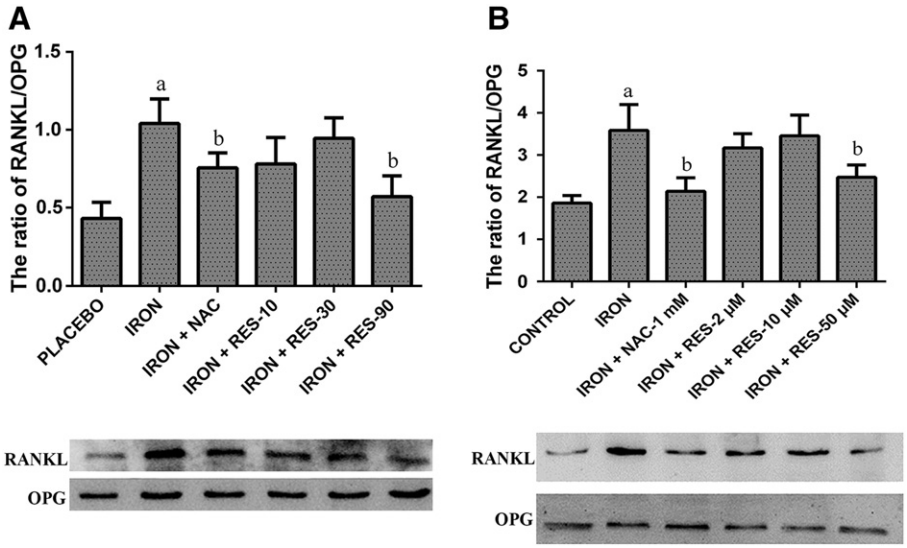

Fig. 5. The effect of RES on the ratio of RANKL to OPG in iron-overload mice and MC3T3-E1 cells. The effect of RES on the expression of OPG and RANKL in the femur of the mice and MC3T3-E1 cells were assayed by western blotting. The ratio of RANKL to OPG in the femur of the mice (A) and MC3T3-E1 cells (B) are represented as the mean±S.D. (n=5) a: P<.05 compared to the control group; b: P<.05 compared to the iron-treated group; c: P<.01 compared to the iron-treated group.

expression of the bone phenotypic protein genes, including osteocalcin, osteopontin and Col I, during osteoblastic differentiation [34]. Osteocalcin, a marker of bone formation, is secreted solely by osteoblasts and is implicated in bone mineralization. In our previous study, ROS significantly suppressed nuclear Runx2 phosphorylation and the expression of Col I in calvarial osteoblasts [35].

Osteoblasts can also produce RANKL and OPG to modulate the formation and differentiation of osteoclasts. As OPG inhibits

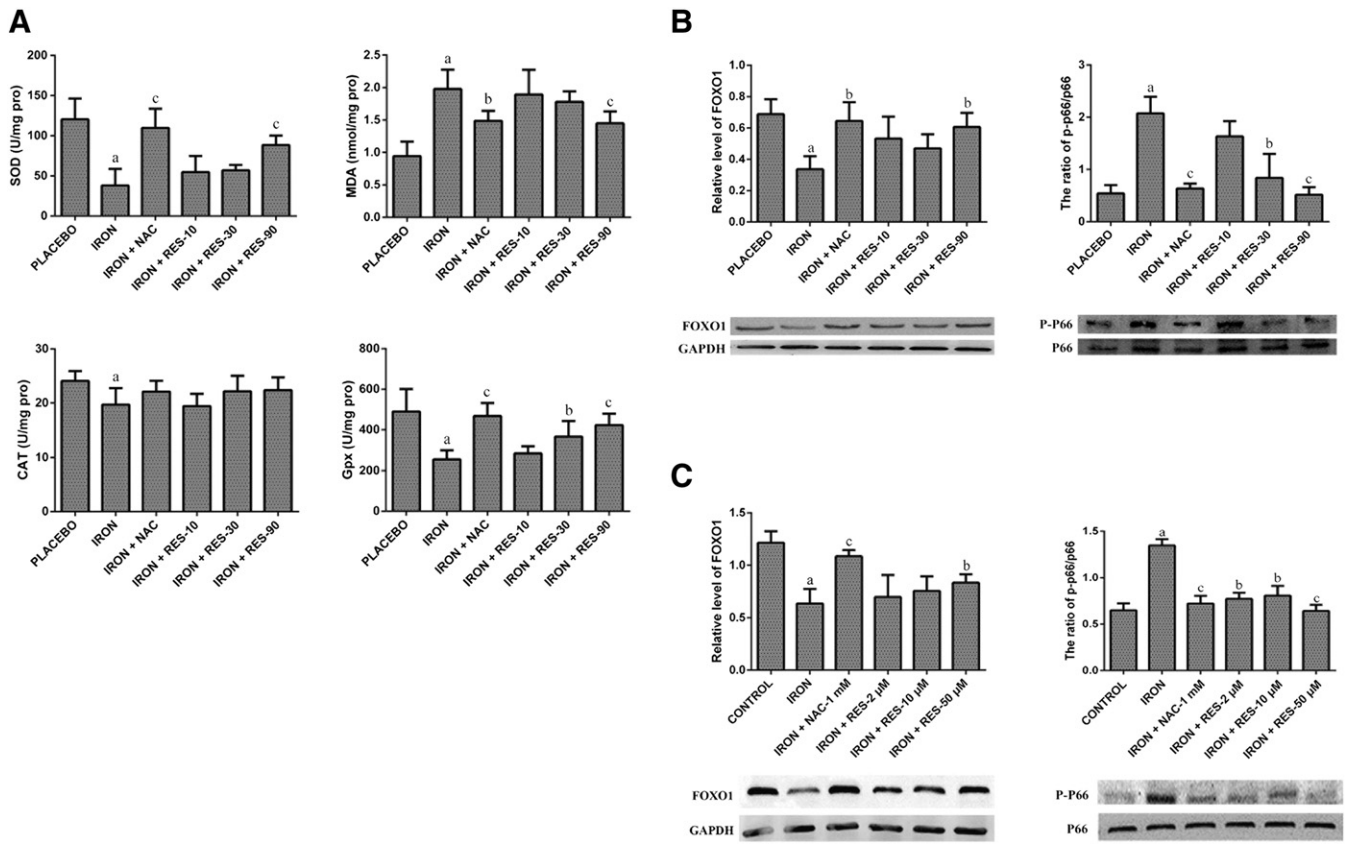

Fig. 6. The antioxidant effect of RES in iron-overload mice and MC3T3-E1 cells. The expressions of FOXO1 and phosphorylation of $p66^{shc}$ in the femur of the mice (A) and MC3T3-E1 cells (C) were assayed by western blotting. Results are represented as the mean±S.D. (n=5) The activities of antioxidant enzymes (B) SOD, CAT and GPx and the concentration of MDA were assayed according to the instructions of the manufacturer. Results are represented as the mean±S.D. (n=10) a: P<.05 compared to the control group; b: P<.05 compared to the iron-treated group; c: P<.01 compared to the iron-treated group.

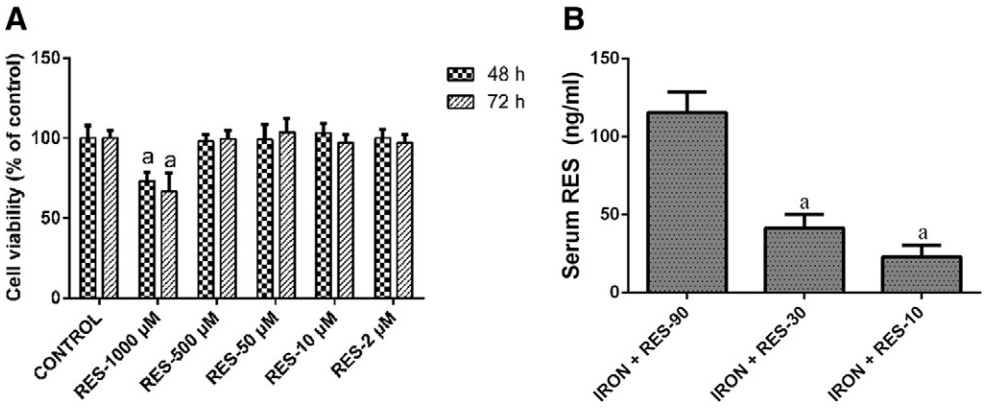

Fig. 7. The vitro cytotoxicity and plasma levels of RES. In MC3T3-E1 cell, the toxicity of RES (2–1000 μM) was determined by MTT assay (A). Results are represented as the mean±S.D. (n=10) a: P<.05 compared to the control group. The blood RES concentrations were measured by UPLC/MS/MS (B). Results are represented as the mean±S.D. (n=8) a: P<.05 compared to high-dose RES group.

osteoclastogenesis while RANKL supports bone resorption of osteoclasts, the ratio of OPG/RANKL is a critical factor in osteoclast differentiation and subsequent bone resorption. Bone remodeling is mainly controlled by the balance of RANKL/OPG, and different modifications in the RANKL/OPG ratio can induce either an excessive bone resorption or, by contrast, excessive bone formation [36]. RANKL binds to its cognate receptor RANK to induce NF-κB activation, leading to osteoclast differentiation, activation and maturation. ROS play an important role in osteoclast differentiation through NF-κB regulation [37]. ROS have been reported to increase in response to RANKL and to act as intracellular second messengers for osteoclastogenesis. ROS produced in macrophages and monocytes through RANKL-TRAF6-Rac1-NADPH oxidase–dependent pathways may be involved in mediation of osteoclast differentiation [38]. Iron overload induced a significant decline in biochemical markers of bone formation as well as enhanced osteoclastogenesis through the OPG/RANKL signaling pathway. In our study, RES significantly down-regulated protein expression of RANKL and maintained the normal level of OPG in mice or MC3T3-E1 cells. In addition, RES can also decrease the serum levels of IL-6, TNF-α and TRACP-5b in the serum of mice under iron-overload conditions. IL-6 and TNF-α not only directly stimulate osteoclastogenesis and bone resorption but also have an important effect on stimulating RANKL production by osteoblastic cells in a synergistic fashion [36]. The concentrations in the serum of IL-6 and TNF-α are associated with increased ROS and increased resorption [39]. TRACP-5b was used as the bone resorption marker because TRACP-5b has the least significant change and minimum significant change and has extremely low interday and intraday variation [40].

Animal experiments have shown that iron overload resulted in osteoporosis combined with renal dysfunction and liver iron-overload syndrome by ROS [41]. ROS induced by H_2O_2 [35], antimycin A [42] or iron [9] can inhibit cell proliferation, differentiation, maturation and mineralization in osteoblasts. In our study, iron accumulated in the serum, liver and spleen of mice after treatment with intraperitoneal iron dextran once a week for 3 months (data not shown). Meanwhile, the activities of CAT, SOD and GPx in the liver of the iron-overload mice decreased significantly, and the level of MDA was significantly elevated in the mice. RES significantly restored hepatic CAT, SOD and GPx and significantly decreased the level of MDA. Various forms of SOD catalyze the conversion of superoxide free radical to H_2O_2, and CAT converts H_2O_2 into water and oxygen. GPx converts peroxides into harmless alcohols in a reaction in which it oxidizes GSH to the disulfide GSSH. FOXOs, characterized by the presence of a winged-helix DNA binding domain called forkhead box, represent a critical cell defense mechanism against oxidative insults [23]. Oxidative stress promotes the translocation of FOXOs into the nucleus and the posttranslational modifications including phosphorylation, ubiquitylation and acetylation [43]. These changes in turn lead to activation of FOXOs and thereby affect FOXO-mediated oxidative stress responses by regulating the transcription of antioxidant enzymes. $p66^{shc}$ is an amplifier of H_2O_2 generation in mitochondria and works as an essential mediator of the stimulating effects of oxidative stress on NF-κB activation, cytokine production and osteoclastogenesis in bone [10].

The suppression of bone formation can be largely prevented by treatment with the antioxidant NAC or RES. NAC is well-known to replenish intracellular glutathione levels to defend against oxidative stress. In our study, excess iron significantly inhibited the expression of FOXO1 in the femur and MC3T3-E1 cells, whereas administration of RES reversed excess-iron-induced inhibition of FOXO1 and the phosphorylation of $p66^{shc}$ to reduce the oxidative damage induced by iron overload. The loss of FOXO1 and the weaker up-regulation of antioxidant enzymes (such as Mn-SOD and CAT [44]) induced by long-term persistent oxidative stress are probably the main factors in bone degeneration. These results suggest that RES may significantly promote osteogenesis via its antioxidant effects. Sirt1 was shown to deacetylate FOXO1, positively regulating FOXO1-dependent gene transcription, and RES enhanced FOXO1 DNA binding at the Rab7 promoter region through a Sirt1-dependent pathway [45]. As a natural Sirt1 activator, RES can suppress $p66^{shc}$ phosphorylation and up-regulate the level of FOXO1 in the bone of mice and osteoblasts under iron-overload conditions. In addition, incubation of osteoblasts with EX-527 reversed the effect of RES on osteogenesis in MC3T3-E1 cells. These findings suggest that antiosteoporosis effect of RES is mediated, at least in part, by activation of Sirt1.

As the advantageous dosages of RES are very narrow, the levels of blood concentrations and toxicity of RES may be obstacles to developing medicines or dietary supplements. The differences in plasma levels of RES among groups treated with 90, 30 or 10 mg/kg RES may result in varying efficacy to protect bone loss induced by excess iron. The advantageous dosages of RES exert antioxidant effect or antiosteoporosis effect and have no toxical effect [46,47]. In addition, RES at the effective dose in our study is nontoxic to MC3T3-E1 cell.

In conclusion, RES protects against excess-iron-induced bone loss mainly by ameliorating the loss of FOXO1 and its antioxidant capacity. These findings imply that RES has potential for developing medicines or dietary supplements to prevent or treat osteoporosis.

Funding

This study was supported by grants from the National Natural Science Foundation of China (Grant No. 81274152), the Natural

Science Foundation of Shanghai Science and Technology Commission, China (Grant No. 13ZR1449600) and the Scientific Research Fund of Shanghai City Health Planning Commission, China (Grant No. 2013299).

References

[1] Moriwaki S, Suzuki K, Muramatsu M, Nomura A, Inoue F, Into T, et al. Delphinidin, one of the major anthocyanidins, prevents bone loss through the inhibition of excessive osteoclastogenesis in osteoporosis model mice. PLoS One 2014;9: e97177.
[2] Jian J, Pelle E, Huang X. Iron and menopause: does increased iron affect the health of postmenopausal women? Antioxid Redox Signal 2009;11:2939–43.
[3] Clemons M, Goss P. Estrogen and the risk of breast cancer. N Engl J Med 2001;344: 276–85.
[4] Yang Q, Jian J, Abramson SB, Huang X. Inhibitory effects of iron on bone morphogenetic protein 2-induced osteoblastogenesis. J Bone Miner Res 2011;26: 1188–96.
[5] Johnson M, Fischer J, Bowman B, Gunter E. Iron nutriture in elderly individuals. FASEB J 1994;8:609–21.
[6] Tsay J, Yang Z, Ross FP, Cunningham-Rundles S, Lin H, Coleman R, et al. Bone loss caused by iron overload in a murine model: importance of oxidative stress. Blood 2010;116:2582–9.
[7] Liu G, Men P, Kenner GH, Miller SC. Therapeutic effects of an oral chelator targeting skeletal tissue damage in experimental postmenopausal osteoporosis in rats. Hemoglobin 2008;32:181–90.
[8] Jomova K, Valko M. Advances in metal-induced oxidative stress and human disease. Toxicology 2011;283:65–87.
[9] Yamasaki K, Hagiwara H. Excess iron inhibits osteoblast metabolism. Toxicol Lett 2009;191:211–5.
[10] Almeida M, Han L, Ambrogini E, Bartell SM, Manolagas SC. Oxidative stress stimulates apoptosis and activates NF-kappaB in osteoblastic cells via a PKCbeta/ p66shc signaling cascade: counter regulation by estrogens or androgens. Mol Endocrinol 2010;24:2030–7.
[11] Vijayan V, Khandelwal M, Manglani K, Singh RR, Gupta S, Surolia A. Homocysteine alters the osteoprotegerin/RANKL system in the osteoblast to promote bone loss: pivotal role of the redox regulator forkhead O1. Free Radic Biol Med 2013;61C: 72–84.
[12] Fernández-Mar MI, Mateos R, García-Parrilla MC, Puertas B, Cantos-Villar E. Bioactive compounds in wine: resveratrol, hydroxytyrosol and melatonin: a review. Food Chem 2012;130:797–813.
[13] Wenzel E, Somoza V. Metabolism and bioavailability of trans-resveratrol. Mol Nutr Food Res 2005;49:472–81.
[14] Artsi H, Cohen-Kfir E, Gurt I, Shahar R, Bajayo A, Kalish N, et al. The Sirtuin1 activator SRT3025 down-regulates sclerostin and rescues ovariectomy-induced bone loss and biomechanical deterioration in female mice. Endocrinology 2014; 155:3508–15.
[15] Hori YS, Kuno A, Hosoda R, Horio Y. Regulation of FOXOs and p53 by SIRT1 modulators under oxidative stress. PLoS One 2013;8:e73875.
[16] Yun J-M, Chien A, Jialal I, Devaraj S. Resveratrol up-regulates SIRT1 and inhibits cellular oxidative stress in the diabetic milieu: mechanistic insights. J Nutr Biochem 2012;23:699–705.
[17] Durbin SM, Jackson JR, Ryan MJ, Gigliotti JC, Alway SE, Tou JC. Resveratrol supplementation preserves long bone mass, microstructure, and strength in hindlimb-suspended old male rats. J Bone Miner Metab 2014;32:38–47.
[18] Shakibaei M, Shayan P, Busch F, Aldinger C, Buhrmann C, Lueders C, et al. Resveratrol mediated modulation of Sirt-1/Runx2 promotes osteogenic differentiation of mesenchymal stem cells: potential role of Runx2 deacetylation. PLoS One 2012;7:e35712.
[19] Shen GS, Yang Q, Jian JL, Zhao GY, Liu LL, Wang X, et al. Hepcidin1 knockout mice display defects in bone microarchitecture and changes of bone formation markers. Calcif Tissue Int 2014;94:632–9.
[20] Jia P, Xu YJ, Zhang ZL, Li K, Li B, Zhang W, et al. Ferric ion could facilitate osteoclast differentiation and bone resorption through the production of reactive oxygen species. J Orthop Res 2012;30:1843–52.
[21] Melville KM, Kelly NH, Khan SA, Schimenti JC, Ross FP, Main RP, et al. Female mice lacking estrogen receptor-alpha in osteoblasts have compromised bone mass and strength. J Bone Miner Res 2014;29:370–9.
[22] Cao Q, Zhang J, Liu H, Wu Q, Chen J, Chen G-Q. The mechanism of anti-osteoporosis effects of 3-hydroxybutyrate and derivatives under simulated microgravity. Biomaterials 2014;35:8273–83.
[23] Manolagas SC. From estrogen-centric to aging and oxidative stress: a revised perspective of the pathogenesis of osteoporosis. Endocr Rev 2010;31: 266–300.
[24] Ruiz-Larrea MB, Leal AM, Liza M, Lacort M, de Groot H. Antioxidant effects of estradiol and 2-hydroxyestradiol on iron-induced lipid peroxidation of rat liver microsomes. Steroids 1994;59:383–8.
[25] Huang W, Shang WL, Wang HD, Wu WW, Hou SX. Sirt1 overexpression protects murine osteoblasts against TNF-alpha-induced injury *in vitro* by suppressing the NF-kappaB signaling pathway. Acta Pharmacol Sin 2012;33:668–74.
[26] Li K, Ma S, Li Y, Ding G, Teng Z, Liu J, et al. Effects of PEMF exposure at different pulses on osteogenesis of MC3T3-E1 cells. Arch Oral Biol 2014;59:921–7.
[27] Li F, Yang Y, Zhu P, Chen W, Qi D, Shi X, et al. Echinacoside promotes bone regeneration by increasing OPG/RANKL ratio in MC3T3-E1 cells. Fitoterapia 2012; 83:1443–50.
[28] Rittling SR, Feng F. Detection of mouse osteopontin by western blotting. Biochem Biophys Res Commun 1998;250:287–92.
[29] Gertz M, Fischer F, Nguyen GTT, Lakshminarasimhan M, Schutkowski M, Weyand M, et al. Ex-527 inhibits Sirtuins by exploiting their unique NAD+-dependent deacetylation mechanism. Proc Natl Acad Sci 2013;110:E2772–81.
[30] Beaumont C, Delaby C. Recycling iron in normal and pathological states. Seminars in hematology, 61. Elsevier; 2009 328–38.
[31] Vijayan V, Khandelwal M, Manglani K, Ranjan Singh R, Gupta S, Surolia A. Homocysteine alters osteoprotegerin/RANKL system in the osteoblast to promote bone loss: pivotal role of redox regulator forkhead O1. Free Radic Biol Med 2013; 61:72–84.
[32] Ishii K-a, Fumoto T, Iwai K, Takeshita S, Ito M, Shimohata N, et al. Coordination of PGC-1β and iron uptake in mitochondrial biogenesis and osteoclast activation. Nat Med 2009;15:259–66.
[33] Zarjou A, Jeney V, Arosio P, Poli M, Zavaczki E, Balla G, et al. Ferritin ferroxidase activity: a potent inhibitor of osteogenesis. J Bone Miner Res 2010;25:164–72.
[34] Nishimura R, Hata K, Harris SE, Ikeda F, Yoneda T. Core-binding factor alpha 1 (Cbfa1) induces osteoblastic differentiation of C2C12 cells without interactions with Smad1 and Smad5. Bone 2002;31:303–12.
[35] Wang Y, Zhao L, Wang Y, Xu J, Nie Y, Guo Y, et al. Curculigoside isolated from *Curculigo orchioides* prevents hydrogen peroxide-induced dysfunction and oxidative damage in calvarial osteoblasts. Acta Biochim Biophys Sin 2012;44: 431–41.
[36] Steeve KT, Marc P, Sandrine T, Dominique H, Yannick F. IL-6, RANKL, TNF-alpha/IL-1: interrelations in bone resorption pathophysiology. Cytokine Growth Factor Rev 2004;15:49–60.
[37] Wauquier F, Leotoing L, Coxam V, Guicheux J, Wittrant Y. Oxidative stress in bone remodelling and disease. Trends Mol Med 2009;15:468–77.
[38] Lee NK, Choi YG, Baik JY, Han SY, Jeong DW, Bae YS, et al. A crucial role for reactive oxygen species in RANKL-induced osteoclast differentiation. Blood 2005;106: 852–9.
[39] Jagger CJ, Lean JM, Davies JT, Chambers TJ. Tumor necrosis factor-alpha mediates osteopenia caused by depletion of antioxidants. Endocrinology 2005;146:113–8.
[40] Lee S, Kumagai T, Hashimoto J, Satoh A, Suzuki T, Yamai K, et al. A change of osteocalcin (OC) and tartrate resistant acid phosphatase 5b (TRACP-5b) with the menstrual cycle. Horm Metab Res 2012;44:699–703.
[41] Kudo H, Suzuki S, Watanabe A, Kikuchi H, Sassa S, Sakamoto S. Effects of colloidal iron overload on renal and hepatic siderosis and the femur in male rats. Toxicology 2008;246:143–7.
[42] Lee YS, Choi EM. Actein isolated from black cohosh promotes the function of osteoblastic MC3T3-E1 cells. J Med Food 2014;17:414–23.
[43] van der Horst A, Burgering BM. Stressing the role of FoxO proteins in lifespan and disease. Nat Rev Mol Cell Biol 2007;8:440–50.
[44] Huang H, Tindall DJ. Dynamic FoxO transcription factors. J Cell Sci 2007;120: 2479–87.
[45] Wang B, Yang Q, Sun YY, Xing YF, Wang YB, Lu XT, et al. Resveratrol-enhanced autophagic flux ameliorates myocardial oxidative stress injury in diabetic mice. J Cell Mol Med 2014;18:1599–611.
[46] Zhao H, Li X, Li N, Liu T, Liu J, Li Z, et al. Long-term resveratrol treatment prevents ovariectomy-induced osteopenia in rats without hyperplastic effects on the uterus. Br J Nutr 2014;111:836–46.
[47] Dumont M, Wille E, Stack C, Calingasan NY, Beal MF, Lin MT. Reduction of oxidative stress, amyloid deposition, and memory deficit by manganese superoxide dismutase overexpression in a transgenic mouse model of Alzheimer's disease. FASEB J 2009;23:2459–66.